Interplay of electron-phonon interaction and Rashba spin-orbit coupling in the Kane-Mele model

I.V. Sankar, Soma Mukhopadhyay, Sankararao Yadam, Raghavendra Kulkarni, C. Hari Krishna

Physics Division, Department of H&S, CVR College of Engineering, Ibrahimpatnam, Ranga Reddy, Telangana 501510, India

E-mail: ivshankar27@gmail.com

Abstract

The quantum phase transition from mobile to immobile polaron within the framework of the Kane-Mele-Holstein model is investigated. The phonon degrees of freedom in the model are eliminated using a variational ansatz based on modified Lang-Firsov transformation within the variational approach to obtain the effective or polaronic Kane-Mele model. The effective model is then studied to understand the effect of electron-phonon interaction on the electronic structure of both bulk graphene and zigzag nanoribbons. The results reveal a significant band renormalization, abrupt (or continuous) nature of the quantum phase transition in the adiabatic (or anti-adiabatic) regime, and the disruption of topological insulating behavior due to strong electron-phonon interaction.

Keywords: Kane-Mele model, topological insulators, electron-phonon interaction, polaron, quantum phase transitions

1. Introduction

The Kane-Mele (KM) model, an archetypical microscopic model for topological insulators (TIs) in two dimensions, was proposed to describe the quantum spin Hall (QSH) effect, an exotic quantum state of matter beyond conventional insulators, metals, and semiconductors, in graphene [1,2]. The QSH state is characterized by an insulating bulk band gap and counter-propagating spin-polarized edge states protected by time-reversal (TR) symmetry [1,2-5]. In the absence of TR breaking perturbations, these robust helical edge states emerge due to prohibited elastic backscattering, resulting in dissipationless spin currents. This makes the KM model fundamental for advancing spintronics, valleytronics, and quantum computations [6-9]. Consequently, the edge states remain resilient against nonmagnetic disorder, preserving dissipationless transport, a hallmark of nontrivial topological quantum phases.

The intrinsic spin-orbit coupling (SOC) in the model gives rise to a topologically nontrivial insulating phase, characterized by helical edge states – electronic states at the boundaries where counter-propagating electrons have opposite spins. This nearest-neighbor SOC couples the spin and momentum, opening the band gap while preserving TR symmetry. It also splits the electronic bands while maintaining TR symmetry, leading to the emergence of a new topological invariant $\mathbb{Z}_2$ index [1,2]. This invariant distinguishes between trivial and topological phases of matter, ensuring the existence of helical edge states that are immune to nonmagnetic disorder. However, real materials are not perfectly isolated systems and there are always quantum lattice fluctuations even at absolute zero temperatures. As a result, the electron-phonon (*e-ph*) interactions play a crucial role in modifying both electronic and topological properties of the system [10-12].

E-ph interactions introduce dynamical lattice fluctuations that can significantly impact the topological phase predicted by the KM model. Phonon-induced electron scattering can significantly renormalize the SOC in the strong *e-ph* interaction regime, potentially suppressing the topological phase by reducing the effect of SOC and driving the system into a trivial insulating phase. In the strong *e-ph* interaction regime, lattice distortions can substantially modify the quantum states, leading to a phase transition between topological and trivial insulating states [13,14]. Certain phonon modes can induce the Peierls-like instability, resulting in gap opening that breaks the topological protection of edge states. This suggests that phonon engineering could be utilized to alter the topological properties in real materials. The formation of polaronic quasiparticles, where electrons become

dressed by a cloud of phonons, affects the carrier mobility and can lead to exotic emergent phenomena such as topological polarons, which may exhibit nontrivial Berry curvature effects [15-18].

The nontrivial topological invariant $\mathbb{Z}_2$ characterizes the system, ensuring the presence of gapless spin-polarized edge states. The *e-ph* and electron-electron (*el-el*) interactions are the two fundamental interactions apart from the SOC. The inclusion of these interactions enriches the phase diagram of the KM model and leads to new quantum phase transitions (QPTs) as a result of competition among the SOC, *e-ph*, *el-el* interactions [19,20]. Previous studies on the interplay between the *e-ph* and *el-el* interactions without SOC suggest that the system can transition into Peierls insulating states for strong *e-ph* interactions, Mott insulating state for strong *el-el* interactions, or metallic state for comparable interaction strengths [19, 22-24].

The *e-ph* interaction leads to the renormalization of charge carriers, which is crucial for understanding the polaronic effects on the transport properties, phonon dispersions, Kohn anomalies, Peierls insulators, charge-density waves, phonon-mediated superconductivity, electrical resistivity, John-Teller distortions, etc. Previous studies have examined *e-ph* interaction effects in tight-binding models (without intrinsic SOC) for graphene, demonstrating polaron formation and its impact on the energy spectrum [25-31]. Certain studies indicate that *e-ph* interaction does not open up a gap at the Dirac point, preserving the gapless helical edge states in the energy spectrum. These studies are significant as they highlight the creation of coherent quasiparticles such as polarons, resulting in substantial renormalization of the effective mass relative to the bare electron mass [32,33]. A thorough understanding of the effect of *e-ph* interaction is essential for developing many-body theories to interpret experimental studies in graphene and other 2D materials with heavier lattices. We refer to the combination of the KM model and Holstein model as a Kane-Mele-Holstein (KMH) model.

Beyond the fundamental aspects, the primary motivation for research in 2D materials lies in their potential for applications in electronic devices. Graphene has limited utility in electronic devices due to its semimetallic nature and perfect transmission of Dirac electrons across the potential barriers, which prevents gate voltage control which is a crucial requirement for conventional field-effect transistor operation. Therefore, opening a band gap in graphene is critical challenge. One potential method is to transform graphene sheets into nanoribbons, where quantum confinement leads to a band gap that scales inversely with ribbon width. To enable transistor functionality at room temperature, a sizable energy gap of 0.5eV is necessary, which can be achieved by reducing the width of nanoribbon to just few nanometers [34,35]. This confinement enhances the electronic properties, making them suitable for practical applications. Our findings reveal the *e-ph* interactions induce a band gap in the zigzag nanoribbons. This effect could be advantageous for electronic devices, as it provides an alternative mechanism for gap engineering beyond quantum confinement. Unfortunately, the formation of polarons reduces the mobility, thereby diminishing electrical conductivity. This occurs because charge carriers become localized due to lattice distortions, making transport less efficient. A thorough understanding of *e-ph* interaction is essential, as it fundamentally limits maximum achievable performance of electronic devices. In this work, we investigate the effects of *e-ph* interaction in both bulk honeycomb lattice and zigzag nanoribbon to explore the resulting physical consequences.

Understanding *e-ph* interactions in the KM model is essential for realizing QSH states in real materials. Graphene's intrinsic SOC is weak, necessitating alternative platforms such asheavy-element graphene analogs, including silicene, germanene, stanene, etc, where *e-ph* interactions play a dominant role. Experimental studies using angle-resolved photoemission spectroscopy, transport measurements have provided insights into phonon-modulated topological phases. Additionally, engineering strain and substrate interactions can serve as external tuning parameters for controlling *e-ph* interaction in topological materials.

The KM model remains a fundamental theoretical framework for understanding topological phases in 2D materials. While it provides an idealized picture of QSH insulators, real-world deviations due to *e-ph* interactions must be carefully considered. The interactions can renormalize SOC, influence edge states stability, and induce topological phase transitions, highlighting the intricate interplay between electronic and lattice degrees of freedom. Investigating these effects is essential for practical realization of topological quantum materials and their applications in low dissipation electronics, spintronics, and valleytronics.

2. Model

The KMH model is given by

$$H = t\sum_{\langle ij\rangle\sigma} c^{\dagger}_{i\sigma}c_{j\sigma} + i\lambda\sum_{\langle\langle ij\rangle\rangle\sigma} \nu_{ij}c^{\dagger}_{i\sigma}\sigma_z c_{j\sigma} + i\lambda_R\sum_{\langle ij\rangle\sigma} c^{\dagger}_{i\sigma}(\boldsymbol{\sigma}\times\boldsymbol{d}_{ij})_z c_{j\sigma} + \epsilon\sum_i \xi_i c^{\dagger}_{i\sigma}c_{j\sigma} + \mathrm{g}\sum_{i\sigma} n_{i\sigma}\left(b_i + b_i^{\dagger}\right) + \omega\sum_i b_i^{\dagger}b_i \quad (1)$$

where $c^{\dagger}_{i\sigma}(c_{i\sigma})$ is the elctron creation (annihilation) operator for π-electron states at site-i with spin σ and $b_i^{\dagger}\ (b_i)$ is the phonon creation (annihilation) operator at site-i. The first term is the nearest-neighbor (NN) hopping term on the honeycomb lattice with hopping probability amplitude t. The NN vectors $\boldsymbol{a_1} = \frac{a}{2}(-\sqrt{3}, -1)$, $\boldsymbol{a_2} = a(0, 1)$, and $\boldsymbol{a_3} = \frac{a}{2}(\sqrt{3}, -1)$ represents the

vectors from a sublattice site $\boldsymbol{A}$ to its three NN sublattice sites $\boldsymbol{B}$. The second term is the mirror-symmetric spin-dependent next NN hopping with the complex hopping amplitude $i\lambda$. Here, $\nu_{ij} = \frac{2}{\sqrt{3}}(\hat{\boldsymbol{d}}_1 \times \hat{\boldsymbol{d}}_2) = \pm 1$, where i and j are next NNs, $\hat{\boldsymbol{d}}_1$ and $\hat{\boldsymbol{d}}_2$ are unit vectors along the two bonds that connect i and j, and σ_z is the Pauli matrix describing the spin of an electron. The vectors between the nearest same sublattice sites are $\boldsymbol{b_1} = \boldsymbol{a_2} - \boldsymbol{a_3}$, $\boldsymbol{b_2} = \boldsymbol{a_3} - \boldsymbol{a_1}$, and $\boldsymbol{b_3} = \boldsymbol{a_1} - \boldsymbol{a_2}$. The third term represents inversion symmetry breaking Rashba SOC with the coupling strength $i\lambda_R$ which may arise due to a perpendicular elecric fieldor interaction with a substrate. The fourth term term describes the staggered sublattice potential ($\xi_i = 1$ for $\boldsymbol{A}$-sublattice sites and $\xi_i = -1$ for $\boldsymbol{B}$-sublattice sites) which violates the symmetry under two-fold rotation in the 2D honeycomb lattice plane. The penultimate term refers to the Holstein-type *e-ph* interaction with interaction strength g. The last term corresponds to the dispersionless free phonons with the phonon frequency ω. We set $\hbar = \omega = \sqrt{3}a = 1$.

The presence of *e-ph* interaction makes makes the KMH Hamiltonian (Eq. 1) too complex to solve exactly so we try to approximately solve it using the variational approach to deal with the phonon degrees of freedom. We first eliminate the phonon degrees of freedomusing the modified Lang-Firsov (LF) transformation to obtain an effective electronic Hamiltonian (Eq. 2) [19,22-24,]. The LF transformation is a coherent state transformation for the phonon subsystem where the coherent strength is determined by the electron density. The conventional LF transformation works very well in the strong couling regime whereas in the weak and intermediate interaction strengths, the lower ground state (GS) energy can be obtained by minimizing the variational GS energy within the framework of modified LF apprach. The generator for the modified LF transformation is given by

$$S = \gamma \mathrm{g} \sum_{i\sigma} n_{i\sigma}(b_i^\dagger + b_i) \tag{2}$$

where γ is a variational parameter. The variational parameter, as expected, depends on all the parameters present in the Hamiltonian. We find that the modified LF transformation gives a better minimum energy than the conventional LF ($\gamma = 1$). We average with zero phonon state $(|0\rangle_{ph})$ after the transformation to obtain the effective or polaronic KM Hamiltonian (after neglecting the induced *el-el* correlations), which is obtained as

$$H = t_{eff} \sum_{\langle ij\rangle\sigma} c_{i\sigma}^\dagger c_{j\sigma} + i\lambda_{eff} \sum_{\langle\langle ij\rangle\rangle\sigma} \nu_{ij} c_{i\sigma}^\dagger \sigma_z c_{j\sigma} + i\lambda_{R,eff} \sum_{\langle ij\rangle\sigma} c_{i\sigma}^\dagger (\boldsymbol{\sigma} \times \boldsymbol{d}_{ij})_z c_{j\sigma} + \epsilon_{eff} \sum_i \xi_i c_{i\sigma}^\dagger c_{j\sigma} \tag{3}$$

where $t_{efff} = te^{-\gamma^2 \mathrm{g}^2}$, $\lambda_{eff} = \lambda e^{-\gamma^2 \mathrm{g}^2}$, $\lambda_{R,eff} = \lambda_R e^{-\gamma^2 \mathrm{g}^2}$, and $\epsilon_{eff} = \epsilon\xi_i - \mathrm{g}^2\gamma(2-\gamma)$ are the effective hopping, intrinsic SOC, RSOC, and on-ste energy terms. From the effective Hamiltonian, we can observe that all the parameters are renormalized which leads to the renormalization of band width and also modifies the on-site energies (which is spin-dependent) in the presence of *e-ph* interaction. This effective Hamiltonian is now basically a polaronic KM Hamiltonian describing the topological aspects of polarons which quasiparticles that are different from the electrons in original KM model. The polaronic KM model is then solved numerically to obtain the results.

3. Results

We first numerically solve the polaronic KM model (Eq. 3) within the conventional LF approach and present the corresponding bulk band structure in Fig. 1 for $k_y = 0$ at various *e-ph* interaction strengths. To isolate the intrinsic influence of *e-ph* interaction on the band structure of the honeycomb lattice, all the other parameters were set to zero except the hopping term. This ensures that any observable modifications to the electronic structure arise solely due to the effect of *e-ph* interaction, eliminating extraneous effects from other interactions. This method allows for a precise analysis of how phonon-induced renormalization impacts the fundamental electronic properties of the system. The result reveals that, as mentioned previously, there is a band renormalization and also a shift in the energy due to the formation of a polaron. These results also reveal that the Dirac cone remains unaffected by the polaron formation but the quasiparticles now have greater effective mass than the bare electrons. The strong renormalization indicates that the charge carriers exhibit a polaronic character.

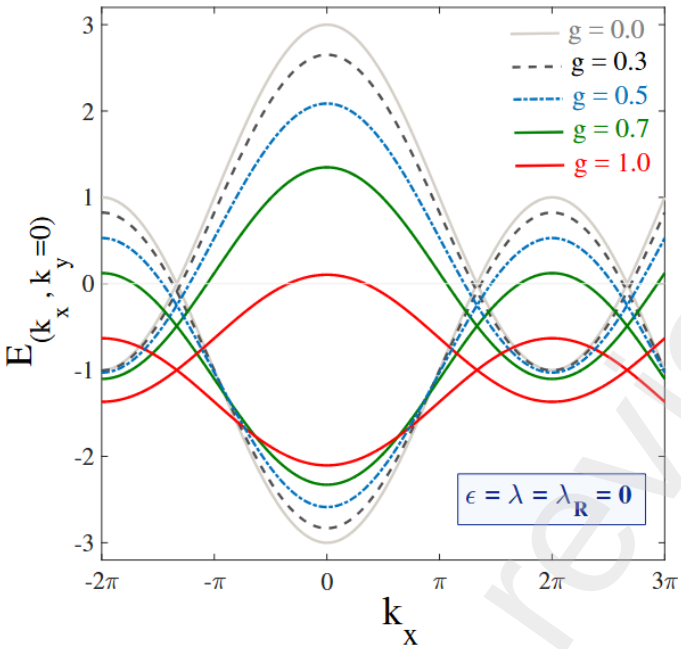

Fig. (1) The band structure of a bulk system for $k_y = 0$ in the conventional LF approach ($\gamma = 1$) for $\epsilon = 0$ at $t = 1$

Now, we solve the polaronic KM model (Eq. 3) within the modified LF approach, which provides an improved description of the phonon subsystem. To obtain the variational GS energy, we numerically minimize the total energy and compared the results with the conventional LF approach. As shown in Fig. 2, the modified LF approach yields a lower GS energy, indicating a more accurate description of the phonon subsystem. The improved variational ansatz, derived from the modified LF transformation, is a better GS for the phonon subsystem and captures the polaronic effects.

The intriguing phenomenon observed in Fig 2 is the emergence of QPT. The system transitions from a mobile or weakly dressed polaron, where the effective hopping amplitude remains comparable to the bare hopping probability amplitude $(t_{eff} \cong t)$, to a strongly localized polaron state, where charge carriers become nearly immobile $(t_{eff} \cong 0)$. This abrupt change (in the adiabatic regime) in t_{eff} signifies the formation of a small polaron due to strong *e-ph* interactions, as the lattice distortions become more pronounced, effectively trapping the charge carriers and suppressing their mobility.

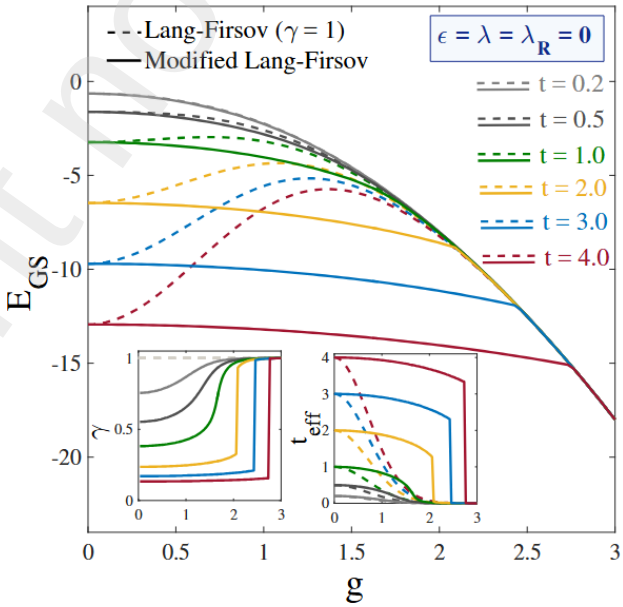

Fig. (2) The variational GS energy (E_{GS}) as a function of *e-ph* interaction strength (g) for various values of hopping (t)

The increased mass of the quasiparticle reduces mobility. In general, the KM model is a four-band model and these four bands originate from the four degrees of freedom: two sublattices (**A** and **B**) and two spins (↑ and ↓). The four bands are spin-up and spin-down bands for **A**-sublattice and **B**-sublattices. In Fig.1, only two bands (each band is doubly-degenerate) appear since $\lambda_R = 0$ and there is a four-fold degeneracy at the Dirac point due to $\epsilon = 0$. We analyze the half-filled band scenario, similar to graphene, where lower band is fully occupied while the upper band remains empty.

In Fig. 2, we also show (in inset) the variation of variational parameter (γ) and the effective hopping probability amplitude (t_{eff}) with the *e-ph* interaction strength, clearly showing the existence of mobile to local polaron QPT as a function of *e-ph* interaction. Though there is a QPT for each hopping amplitude, the nature of the QPT varies depending on the ratio of the hopping amplitude to the phonon frequency. When $t < \omega$ (the anti-adiabatic regime), the phonon dynamics are faster compared to the electron dynamics, the QPT occurs smoothly allowing the system to adapt continuously with increasing *e-ph* interactions while forming polarons. In contrast, when $t > \omega$ (the adiabatic regime), where electrons move faster than the phonons the QPT is abrupt, leading to a sudden localization of charge carriers as the polaron formations becomes energetically favorable. This behavior is consistent with the previous studies on QPTs within the Holstein and Holstein-Hubbard models in one and two-dimensions where similar smooth and abrupt QPTs were observed depending on the adiabaticity of the system [22-24, 37-40]. These finding highlight the fundamental role of phonon dynamics in determining the nature of polaron formation and thus the charge transport.

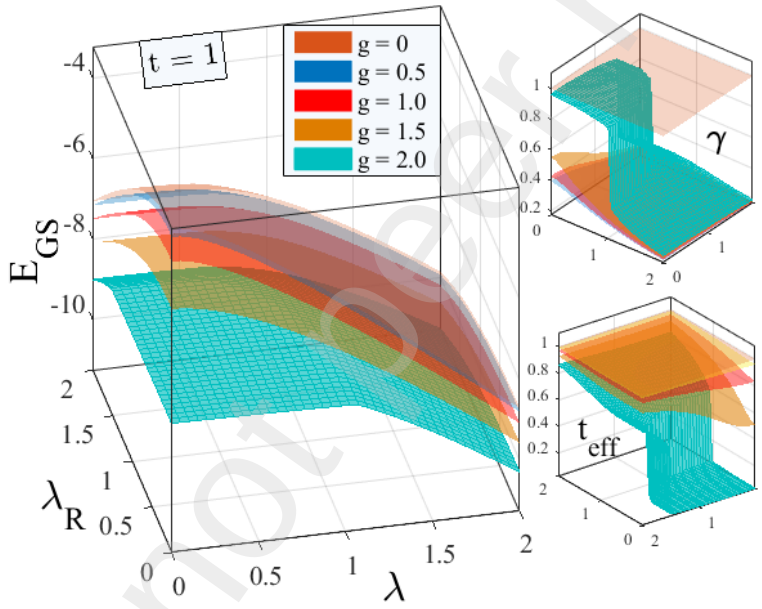

Fig. (3) The variational GS energy (E_{GS}) as a function of λ and λ_R for different values of *e-ph* interaction strength (g) at $\epsilon = 0$ and $t = 1$.

In Fig. 3, we plot the surface diagram of variational GS energy as a function of λ and λ_R. Though the system is already gapped, there exists a polaron transition within a band which implies a quenching of band for certain combinations of parameters (λ, λ_R) i.e., the system is a tougher insulator in the presence of *e-ph* interaction. In other words, to make the system conducting, one needs to provide an external voltage that should overcome both the gap opening terms and the *e-ph* interaction strength. In Fig. 4, we show the band structure within the modified LF approach for both the bulk and zigzag edge states. From now on, we will consistently present our results using the modified Lang-Firsov (LF) approach, as it provides a more accurate representation for the GS. Fig. 4(*a*,*d*) represents the band structure in the absence of both and on-site energy i.e., $\lambda = \lambda_R = 0$ and $\epsilon = 0$. In this scenario, there is a downward shift in the energy band structure due to the formation of polaron. In the presence of small gap opening term $(\epsilon = 0.1)$, which is shown in Fig 4(*b*,*e*), the system exhibits chiral edge states as expected and finally when the on-ste energy is dominent $(\epsilon = 0.5)$, the conducting edge states disppears [1,2].

Next, we investigate the influence of *e-ph* interaction on the edge state of a honeycomb nanoribbon with zigzag edge boundaries. The system is considered periodic along the *x*-direction while with finite boundary in the transverse direction, leading to the presence of two-distinct edges. Due to periodicity, the crystal momentum k_x remains a well-defined quantum number, allowiing us to analyze the electronic state in the momentum space. To capture the effect of *e-ph* on the edge states,

we numerically solve the polaronic KM model under open boundary conditions along the transverse direction. By applying a Fourier transformation along k_x, we reformulate the effective Hamiltonian in momentum space, enabling us a more transparent

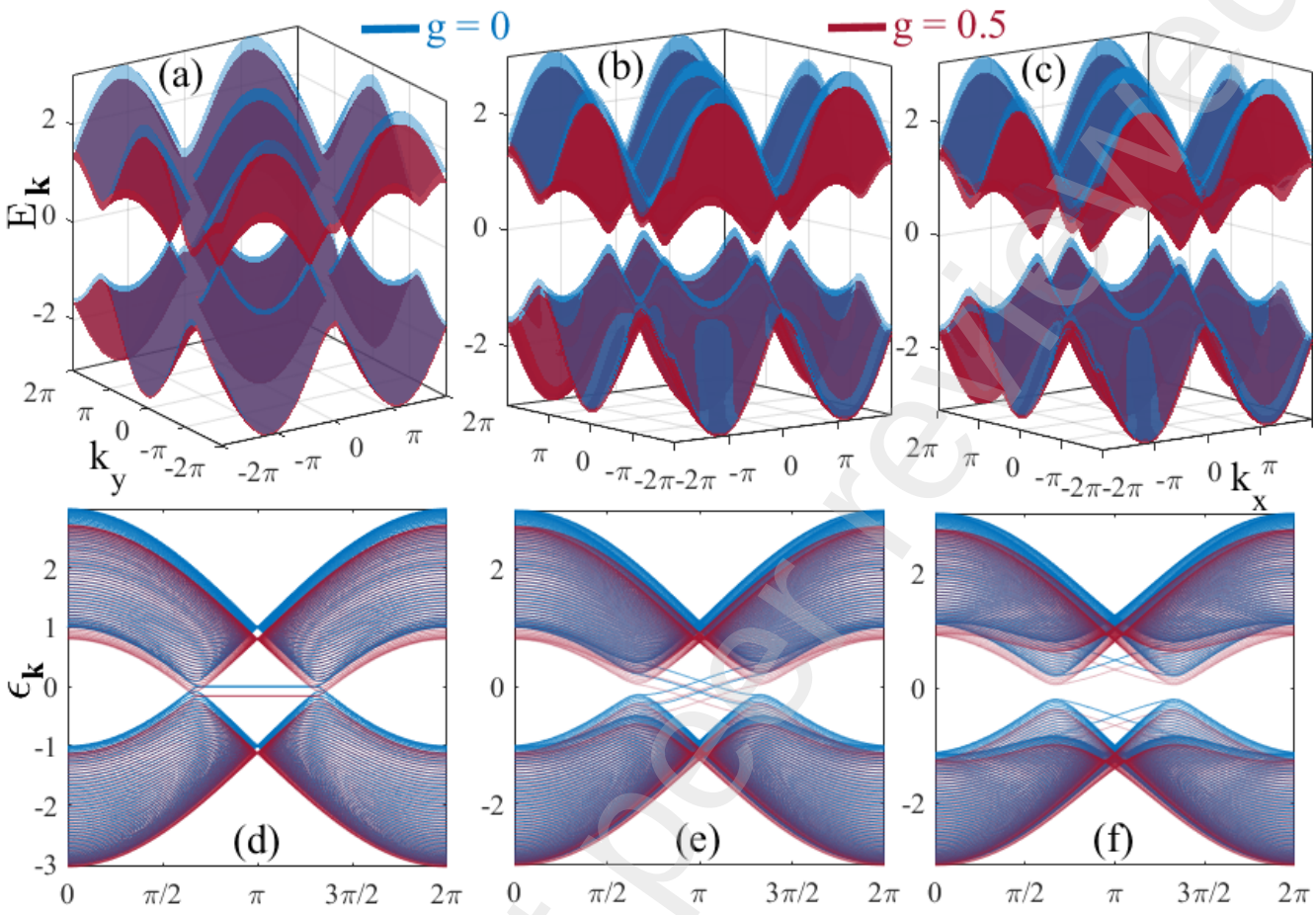

Fig. (4) The bulk band structure $\boldsymbol{E_k}$ and edge states $\boldsymbol{\epsilon_k}$ for (*a,d*) $\epsilon = 0$, $\lambda = 0$, and $\lambda_R = 0$, (*b,e*) $\epsilon = 0.1$, $\lambda = 0.06$, and $\lambda_R = 0.05$, and (*c,f*) $\epsilon = 0.5$, $\lambda = 0.06$, and $\lambda_R = 0.05$.

characterization of the modified band structure and analyze the behavior of the edge states in the presence of the lattice distortions. The corresponding results are shown in Fig. 4 in the presence of *e-ph* interaction for two different values of on-site energies: when $\epsilon = 0.1$, the edge states are conducting whereas for $\epsilon = 0.5$, a gap opens in the edge states. Despite this difference in the edge behavior, the bulk band structure retains a gap in both cases, confirming that the system remains a topological insulator when $\epsilon = 0.1$ for small and intermediate *e-ph* interaction strengths. Notably, in the absence of *e-ph* interaction, our findings align precisely with previous studies [2,41], validating our approach.

The presence of *e-ph* interaction enhances the stability of the system by lowering the GS energy while simultaneously reducing the mobility of the edge states due to band narrowing. Despite this, the edge states remain protected by TR symmetry in the weak and intermediate regimes. For strong *e-ph* interaction, our results indicate that the edge states develop a gap when a finite on-site energy $(\epsilon \neq 0)$ is introduced. However, when $\epsilon = 0$, the edge states remain gapless regardless of the *e-ph* interaction strength. This suggests that while a conducting channel persists between the valence band and conduction bands, the effective hopping amplitude is nearly zero $(t_{eff} \sim 0)$ in the strong *e-ph* interactions, meaning electron transport is significantly suppressed at the Dirac point. Futhermore, for $\epsilon = 0$, sublattice and TR symmetries continue to protect the helical edge states, ensuring their robustness against *e-ph* interaction. In contrast, for $\epsilon \neq 0$, stronger *e-ph* interactions strengthens the impact of the on-site energy, potentially destabilizing the system. This leads to the sublattice symmetry breaking and also break the TR symmetry, leading to the supression of helical edge states (the reason for breaking of TR symmetry is unknown yet). This behavior can also be understood quantitative by analyzing the effective on-site energy term:

$$\epsilon_{eff} = \epsilon\xi_i - g^2\gamma(2-\gamma) \quad (4)$$

When $\epsilon = 0$, there is no competition between the bare on-site energy and the *e-ph* interaction-enhanced energy shift. In this case, both **A** and **B**-sublattice sites acquire the same effective on-site energy $(\epsilon_{eff} < 0)$, ensuring that sublattice symmetry

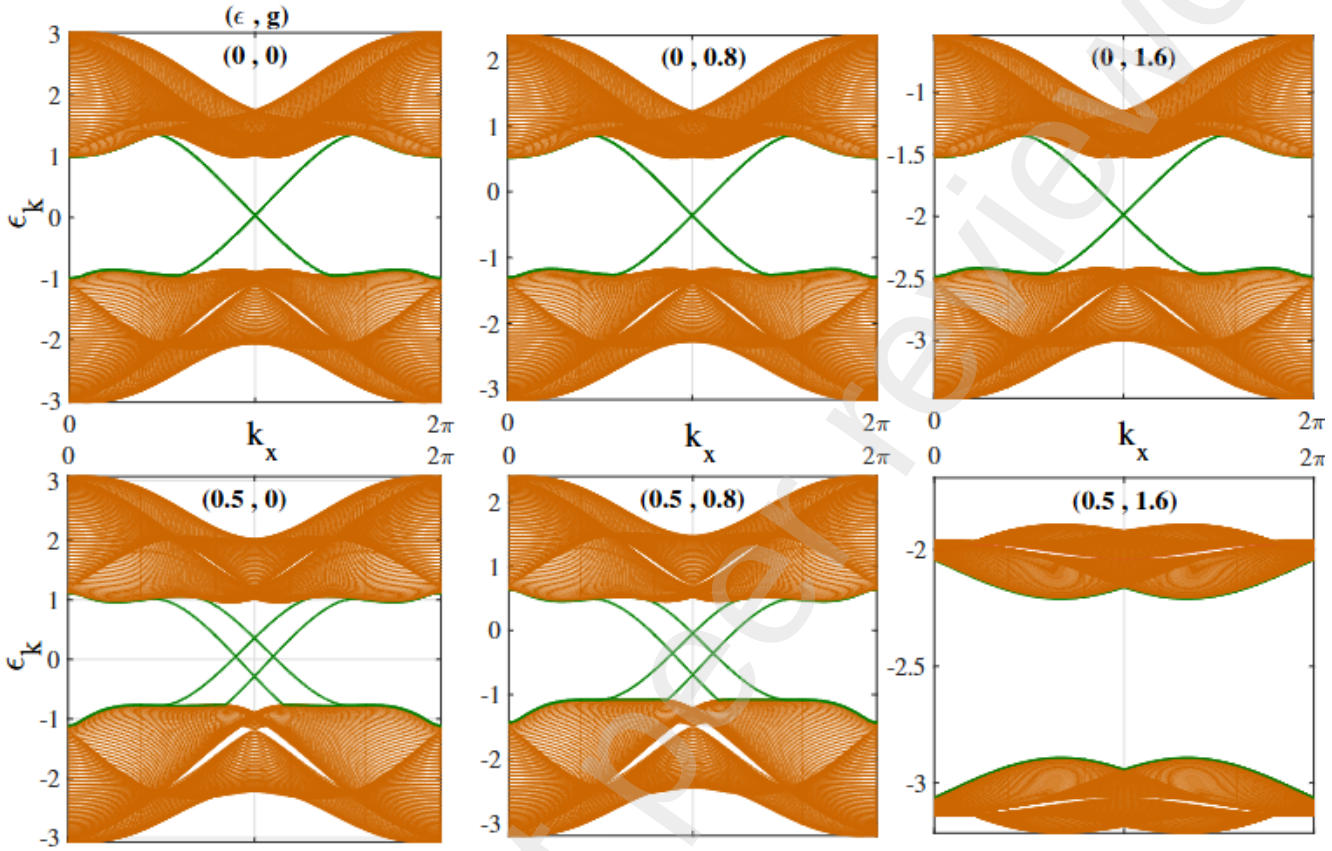

Fig. (5) The edge states for $\lambda = 0.3$ and $\lambda_R = 0.2$ at $t = 1$ for zigzag nanoribbon with $N = 50$.

remains intact. Consequently TR symmetry continues to protect the helical edge states, maintaining their gapless nature. However, $\epsilon \neq 0$, the effective on-site energy differs between the two sublattices, leading to sublattice symmetry breaking. This symmetry breaking becomes more pronounced as the *e-ph* interaction strengthens, potentially destabilizing the helical edge states. In this regime, the interplay between on-site energy and *e-ph* interaction distrupts the TR symmetry, ultimately the emergence of a gap in the edge states, as discussed previously and illustrated in Fig. (5).

In Fig. 6, we analyze the interplay between RSOC and *e-ph* interactions, focusing on the combined impact on the electronic and topological properties. It is well established that RSOC enhances electronic mobility by increasing the effective hopping amplitudes, thereby preventing significant bandwidth narrowing. This effect arises because RSOC introduces spin-momentum locking in the presence of inversion asymmetry, leading to spin-split bands that reduce localization effects. However, despite the enhanced mobility induced by RSOC, our results predicts a universal transition from a metallic state to insulating state as the strength of the *e-ph* interaction increases. This transition suggests that polaron formation in strong e-ph interaction regimes dominates over the delocalizing effects due to RSOC, leading to small polaron formation and suppressed conductivity. Moreover, we observe that for all values of RSOC, the helical edge states are absent in the strong *e-ph* interaction regime. This suggests a fundamental instability in the QSH insulating phase, likely due to the breakdown of TR symmetry or sublattice symmetry caused by phonon-mediated renormalization of the effective on-site energies.

The presence of helical edge states in a topological insulator is typically protected by TR symmetry, ensuring that counterpropagating edge states with opposite spins remain robust against nanomagnetic disorder. However, in the presence of strong *e-ph* interactions, this protection appears to be lost, possibly due to phonon-induced backscattering, which can lift the topological protection by dynamically breaking TR symmetry. Additionally, in conventional Rashba-dominated systems, one might expect enhanced conductivity, yet our findings indicate that even strong RSOC cannot counteract the localization effects

induced by strong *e-ph* interaction. This confirms that the topological insulating state is fragile under strong *e-ph* interactions, independent of whether magnetic impurity or external magnetic fields are present. Our results predict that sufficient strong *e-ph* interactions can induce a phonon-driven topological phase transition, ultimately destroying the topological insulating nature and suppressing helical edge transport.

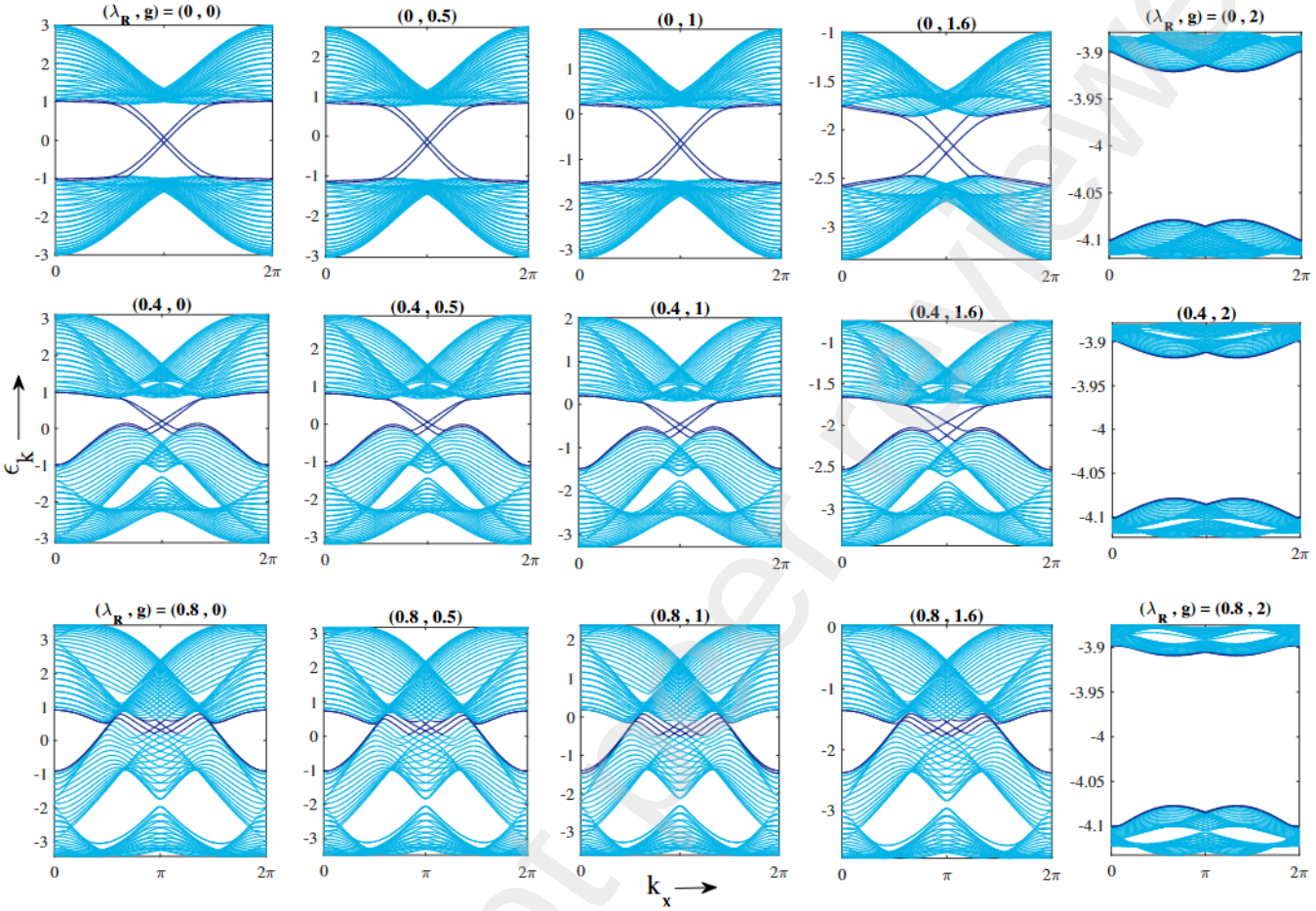

Fig. (6) The edge states for $\lambda = 0.2$ and $\epsilon = 0.1$ at $t = 1$ for the zigzag nanoribbon with $N = 20$.

Conclusions

We have investigated the effect of *e-ph* interaction within the framework of the Kane-Mele-Holstein model. To eliminate phonon degrees of freedom, we applied the modified Lang-Firsov transformation followed by a zero phonon averaging. This approach yields a polaronic version of the Kane-Mele model, which we then numerically solved to examine the transition from a mobile to a localized polaronic state. For both bulk honeycomb lattices and zigzag nanoribbons, our results indicate the formation of localized polarons. The transition from a free polaron state to a localized polaron state occurs smoothly in the anti-adiabatic regime ($t < \omega$), where phonons respond quickly to electronic motion. In contrast, in the adiabatic regime ($t > \omega$), where the electron motion is dominant, the transition is abrupt, signifying strong polaron localization. Notably, we also found that strong *e-ph* interactions induce a gap in the zigzag edge states, effectively destroying the topological insulating behavior of the system. This breakdown occurs as the strong *e-ph* interaction localizes charge carriers, thus formation immobile small polarons, disrupting the symmetry-protected edge conduction that defines the topological phase. As a result, the system transitions from a topological insulator to a trivial insulating state, where edge transport is no longer protected. This finding highlights the crucial role of *e-ph* interactions in destabilizing topological order and could provide new avenues for engineering topological phase transitions in real materials and also posing fundamental limitations for topological materials in realistic, interacting environments.

Declaration of generative AI and AI-assisted technologies in the writing process

During the preparation of this work the authors utilized ChatGPT to assist with correcting typographical errors, improving grammar, and enhancing the clarity. After using this tool/service, the authors reviewed and edited the content as needed and take full responsibility for the content of the publication.

References

[1] Kane C L and Mele E J 2005 *Phys. Rev. Lett.* **95**, 146802
[2] Kane C L and Mele E J 2005 *Phys. Rev. Lett.* **95**, 226801
[3] Bernevig B A., Hughes T L., and Zhang S -C, 2006 *Science* **314**, 1757-1761
[4] Ghiasi T S, et al. 2024 *Nano Lett.* **24**, 1234-1240 (2024)
[5] Kang K, et al 2025 *Nano Lett.* **24**, 5678-5684
[6] Gibertini M, Pizzi G, and N. Marzari, 2018 *Phys. Rev. Lett.* **120**, 117701
[7] Pizzochero M, Gibertini M, and Marzari 2024 *Phys. Rev. B* **109**, 165424
[8] Smith A and Jones B 2024 *J. Appl. Phys.* **130**, 074302
[9] He M, Sun H, and He Q L 2019 *Front. Phys.* **14**, 43401
[10] Kim D, Lee S, and Park J 2020 *J. Phys. Chem. Lett.* **11**, 123
[11] Zhang H, Wang L, and Liu Q 2023 *Nano Lett.* **23**, 5678
[12] Jiang Y, Ni J, and Lu J 2024 *Nanoscale* **16**, 1234
[13] Islam M, Battacharyya K, and Basu S 2024 *Phys. Rev. B* **110**, 045426
[14] Budich J C, Dolcini F, Recher P, and Trauzettel B 2012 *Phys. Rev. Lett.* **108**, 086602
[15] Saha K, Garate I 2014 *Phys. Rev. B* **89**, 205103
[16] Grusdt F, Yao N Y, and Demler E A 2019 *Phys. Rev. B* **100**, 075126
[17] Lafuente-Bartolo J, Lian C, and Giustino 2024 *Proc. Natl. Acad. Sci. U.S.A* **121**, e2318151121
[18] Wang Z, Dong L, Xiao, and Niu Q 2021 *Phys. Rev. Lett.* **126** 187001
[19] Takada Y and Chatterjee A 2003 *Phys. Rev. B* **67**, 081102
[20] Costa C C, Seki K, Yunoki S, and Sorella S, 2020 *Commun Phys.* **3**, 80
[21] Werner P and Millis A J 2007 *Phys. Rev. Lett.* **99**, 146404
[22] Sankar I V and Chatterjee A 2012 *Physica C* **480**, 55
[23] Sankar I V and Chatterjee A 2014 *Eur. Phys. J. B* **87**, 154
[24] Sankar I V and Chatterjee A 2016 *Physica B* **489**, 17
[25] Massignan P *et. al.,* 2025 *arXiv:*2501.09618
[26] Sio W H and Giustino F 2023 *Nat. Phys.* **19**, 629
[27] Giustino F 2017 *Rev. Mod. Phys.* **89***,* 15003
[28] Devreese J T and Alexandrov A S 2009 *Rep. Prog. Phys.* **72**, 066501
[29] Alexandrov A S and Devreese J T, Advances in Polaron Physics (Springer-Verlag, Berlin, 1987)
[30] Chatterjee A and Mukhopadhyay, Polarons and Bipolarons: an Introduction (CRC Press, Boca Raton, FL, 2017)
[31] Emin D, Polarons (Cambridge University Press, 2012)
[32] Stauber T and Peres N M R, 2007 *J. Phys.: Condens. Matter* **20**, 055002
[33] Hague J P 2012 *Phys. Rev. B* **86**, 064302
[34] Avouris P, Chen Z, and Perebeinos 2007 *Nat. Nanotechnol.* **2**, 605
[35] Karakachian H *et. al.,* 2020 *Nat. Commun.* **11**, 6380
[36] Fehske H, Ihle D, Loos J, Trapper U, and Buttner H 1993 *Z. Phys.* **94**, 91
[37] Romero A H, Brown H G, and Lindenberg 1999 *Phys. Rev. B* **60**, 4618
[38] Hohenadler M, Evertz H G, and von der Linden W 2004 *Phys. Rev. B* **69**, 024301
[39] Hohenadler M, Evertz H G, and von der Linden W 2005 *Phys. Stat. Sol. B* **242**, 1406
[40] Spencer P E, Samson J H, Kornilovitch P E, and Alexandrov A S 2005 *Phys. Rev. B* **71**, 184310
[41] Wang Z, Hao N, and Zhang P 2009 *Phys. Rev. B* **80**, 115420